

Fig. 2 Height profiles of *a*, the increase in plasma pressure at 21:06 and 21:42 UT on 6 May 1987 (N is the electron concentration and T_e is the electron temperature); *b*, the observed and model values of plasma velocity parallel to the magnetic field line during the two events. Observed values are dots with error bars, and predicted values are solid curves.

In determining the values of $T_{||}$ we have assumed that in the topside of the ionosphere the ion population is dominated by O^+ . During upwelling it is possible that molecular ions might form a significant proportion of the ionospheric plasma at 300 km, in which case the true increase in $T_{||}$ at this height would be even more than our measurements suggest. At greater heights we can be certain that the proportion of molecular ions is negligible, so that if upwelling of molecular ions occurs the effect of plasma pressure will be even stronger than we have calculated.

This observed acceleration is transient, not steady-state. A strong electric field obviously plays a key role, by driving the Pedersen currents which cause Joule heating and an upwelling of the neutral atmosphere. It also drives the ion population at high speed through the neutral atmosphere, which leads to frictional heating and an enhanced gradient of plasma pressure, as well as the formation of an anisotropic ion-velocity distribution which brings the hydrodynamic mirror force into play.

But a strong electric field is not enough in itself; if it were, large upward velocities would be more common. It is also necessary that soft particle precipitation (<1 keV) create sufficient conductivity in the upper E-region for the Joule heating to be intense. On 6 May 1987 such precipitation was indicated by the increased ionization at ~150 km which was observed between a sharp onset at 21:00 and an equally sharp cutoff at 21:48 UT. The degree of frictional heating is also much greater if the neutral velocity is in the opposite direction to the plasma velocity: these conditions occur in the region of the Harang discontinuity, and it is precisely in this region that the large upward velocities reported here were observed.

We acknowledge the constant support of the Director and

Staff at EISCAT. EISCAT is an international facility supported by France, Finland, West Germany, Norway, Sweden and the United Kingdom.

Received 8 August; accepted 10 October 1988.

1. St.-Maurice, J.-P. & Schunk, R. W. *Rev. Geophys. Sp. Phys.* **17**, 99-134 (1979).
2. Lockwood, M. *et al. Geophys. Res. Lett.* **14**, 111-114 (1987).
3. Suvanto, K., Lockwood, M. & Fuller-Rowell, T. G. *J. geophys. Res.* (in the press).
4. Folkestad, K., Hagfors, T. & Westerlund, S. *Radio Sci.* **18**, 867-879 (1983).
5. Winsor, K. J., Jones, G. O. L. & Williams, P. J. S. *Physica Scripta* **37**, 640-644 (1988).
6. Winsor, K. J., Jones, G. O. L. & Williams, P. J. S. *J. atmos. terr. Phys.* **50**, 379-382 (1988).
7. Jones, G. O. L., Winsor, K. J. & Williams, P. J. S. *J. atmos. terr. Phys.* **48**, 887-892 (1986).
8. Smith, R. W., Winsor, K. J., van Eyken, A. P., Quegan, S. & Allen, B. T. *J. atmos. terr. Phys.* **47**, 489-495 (1985).
9. Lockwood, M. *Adv. Sp. Res.* **6**, 63-77 (1982).
10. Winsor, K. J., Jones, G. O. L. & Williams, P. J. S. *J. atmos. terr. Phys.* **48**, 893-904 (1986).
11. Winsor, K. J., Farmer, A., Rees, D. & Aruliah, A. *J. atmos. terr. Phys.* **50**, 369-377 (1988).
12. Burnside, R. G., Tepley, C. A. & Wickwar, V. B. *Ann. Geophys.* **5A**, 343-349 (1987).
13. Hedin, A. *J. geophys. Res.* **92**, 4649-4662 (1987).

Where do channels begin?

David R. Montgomery & William E. Dietrich

Department of Geology and Geophysics, University of California, Berkeley, California 94720, USA

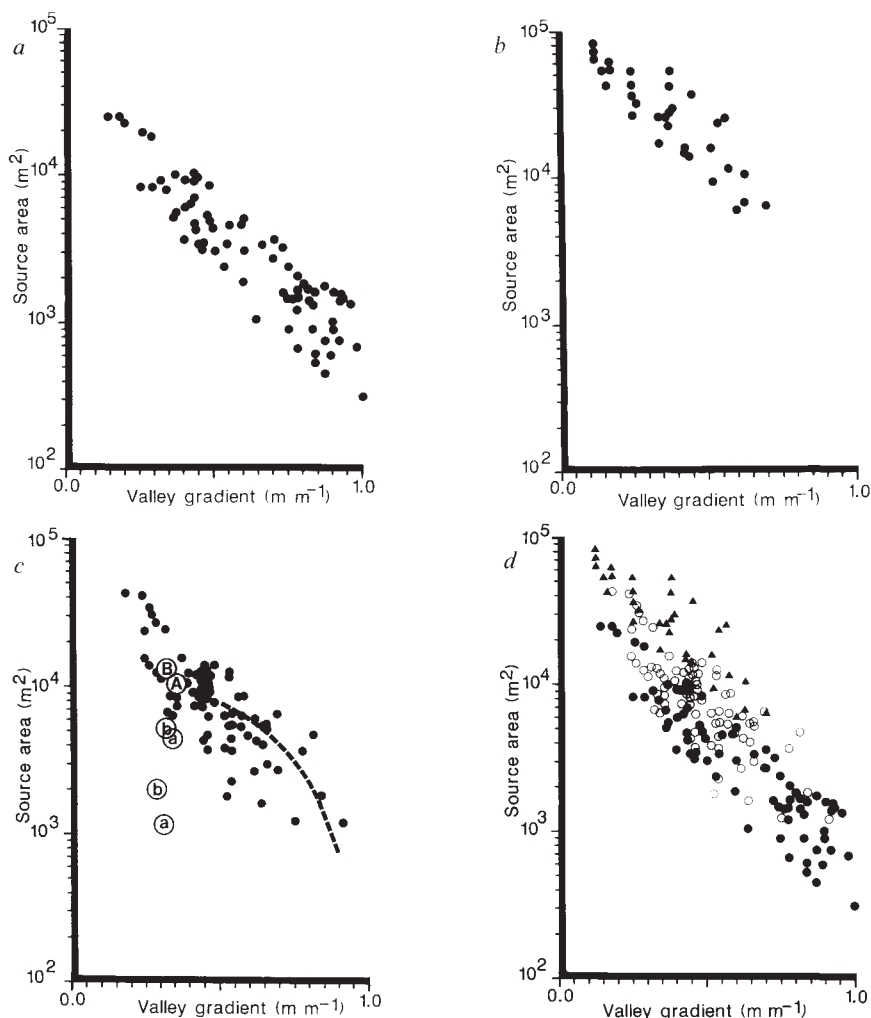
The closer channels begin to drainage divides, the greater will be the number of channels that occupy a unit area, and consequently the more finely dissected will be the landscape. Hence, a key component of channel network growth and landscape evolution theories¹⁻⁷, as well as models for topographically controlled catchment runoff⁸, should be the prediction of where channels begin. Little field data exist, however, either on channel head locations⁹⁻¹⁴ or on what processes act to initiate and maintain a channel¹⁴⁻¹⁷. Here we report observations from several soil-mantled regions of Oregon and California, which show that the source area above the channel head decreases with increasing local valley gradient for slopes ranging from 5 to 45 degrees. Our results support a predicted relationship between source area and slope for steep humid landscapes where channel initiation is by landsliding, but they contradict theoretical predictions for channel initiation by overland flow in gentle valleys. Our data also suggest that, for the same gradient, drier regions tend to have larger source areas.

We selected three areas in Oregon and California for a study of channel-head source areas on the grounds of accessibility, the range of slopes available, and their climatic and geological setting. The Coos Bay, Oregon, study area is located within an actively logged Douglas Fir (*Pseudotsuga menziesii*) forest on private land in the Oregon Coast Range, is underlain by folded Palaeocene basalts and gently dipping Eocene sandstones¹⁸, and receives a mean annual rainfall of ~1,500 mm (ref. 19). Of the 71 channel heads mapped in this area, 19 are associated with small-scale landslide scars, all of which predate recent logging activity. The plot of source area size against the local valley gradient at the channel head indicates a strong inverse correlation (Fig. 1a).

The southern Sierra Nevada study area is composed of two drainage basins on the Rankin Ranch, ~45 km east of Bakersfield, California. The region is covered by open oak woodland and grasslands, is underlain by Cretaceous granitic rocks²⁰ and receives an annual rainfall of ~260 mm (ref. 19). Evidence of previous landsliding and seepage erosion at abrupt channel heads was noted on steeper slopes; channels on gentle slopes, however, generally begin gradually and with evidence of overland flow. Most of the 33 channels mapped in this area begin as discontinuous channel segments. We defined a channel head as the farthest upslope location of a channel with well defined banks. The plot of source area against local hillslope gradient at the channel head for the southern Sierra data (Fig. 1b) also defines a clear inverse relationship. These data differ

Fig. 1 Source area plotted against the local valley gradient, or slope at channel heads, $\tan \theta$, for *a*, Coos Bay, Oregon, *b*, southern Sierra Nevada, California, and *c*, Marin County, California. For the study area in *c*, downslope from the drainage divide in two hollows the slope within the source area is relatively constant (lower case letters in open circles) until the channel begins (capital letters in open circles). The dashed line is the relationship predicted by equation (1). *d*, Combined data from all three field areas, defining a strong inverse linear relation over the full range of data. The southern Sierra data (triangles) generally overlie the Marin County data (open circles) which, in turn, appear to overlie the Coos Bay data (solid circles). This difference is most clearly expressed in the low gradient sites.

Methods. *a*. Channel head surveys were conducted at two recent clear cuts, the larger of which contained drainage basins composed of both low- and high-gradient source areas. The smaller basin consisted of moderately steep source areas in a single drainage basin. Every channel head in both areas was located in the field and mapped onto a 1:4,800 scale topographic basemap. The local hillslope gradient at each channel head was measured by two observers with Brunton compasses to within one degree agreement. Source areas contributing runoff to channel heads were measured with a digital planimeter for each of the three field areas. *b*. Channel head surveys were conducted in two adjacent basins, one of which contained predominantly shallow slopes whereas the other consisted primarily of steeper gradients. Field work used methods identical to those employed in the Coos Bay study area and was mapped onto an enlarged copy of the USGS Oiler Peak 7.5-min quadrangle. *c*. Source areas from three contiguous basins were mapped, using methods identical to those employed in the other study areas, onto an enlarged copy of the USGS Point Bonita 7.5-min quadrangle. Data for the unchannelled areas above channel heads were collected using identical methods. The procedure used to compare equation (1) with field data is discussed in detail in ref. 14 and by D.R.M. and W.E.D. (manuscript in preparation).



from those previously reported for this area¹³ in that the gradients presented here are field measurements of the unchannelled valley floor immediately above channel heads rather than the average slope of the entire source area measured from topographic maps. This distinction is important in that erosional processes controlling channel head locations should be strongly influenced by the local slope. Furthermore, elevations on published topographic maps are only accurate to within one half of the contour interval²¹, which would tend to artificially scatter map-derived data.

The Marin County study area occupies three contiguous drainage basins in the Golden Gate National Recreation Area 10 km north of San Francisco, California. In contrast to the relatively undeformed bedrock of the Coos Bay and southern Sierra areas, this region is underlain by stacked thrust sheets of greenstone, greywacke and chert typical of the Jurassic/Cretaceous Franciscan assemblage in the Marin Headlands terrane²². This area receives an average of 760 mm of rainfall annually²³ and was grazed before the early 1970s. Vegetation presently consists of coastal prairie, northern coastal scrub and introduced species. Of the 80 first-order channels mapped in this area, 49 begin abruptly, generally at small-scale landslide scarps or arcuate tension cracks. The remaining 31 channels begin as discontinuous channel segments with evidence for headcut undermining by seepage erosion. In both cases we defined the channel head location as the point nearest the upslope drainage divide that exhibits evidence of a channelled morphology. The plot of source area against local hillslope

gradient at the channel head for the Marin County data (Fig. 1c) also indicates an inverse relationship.

To test whether the inverse source-area/slope relation is a reflection of the well-known observation that the area of drainage basins increases with decreasing gradient downslope^{9,24}, we determined the area/slope relationship from the drainage divide downslope to the channel head, for two typical Marin County sites (Fig. 1c). The local valley gradient within these source areas is fairly uniform and the drainage area for locations along the topographic axis of both source areas fall below the variance of the data for channel heads. Furthermore, in both cases the channels begin at a point for which the drainage area lies within the scatter of the area/slope relationship for channel heads. These observations suggest that, in general, channels begin at the first point downslope from the drainage divide for which there is sufficient area to support a channel, and that the area/slope relation for drainage basins does not apply upslope of channel heads.

Two quantitative channel initiation theories^{14,25} for semi-arid to humid landscapes have been proposed which predict that source area size should vary as a function of valley gradient. For steep terrain, both theories assume that channel heads are formed by periodic, small-scale landsliding and both predict a rapid decrease in source area size with increasing valley gradient. Because of its analytical form and the limited number of variables it involves, the model by Dietrich *et al.*¹⁴ can be compared with our field results. The model is composed of two parts: a model for shallow sub-surface runoff (based on a theory by

Iida²⁶) and an infinite-slope, Coulomb failure model which, in this case, assumes that the soil is cohesionless at failure. Sub-surface runoff increases pore pressures in the soil, reducing the effective normal stress and consequently the strength of the soil. The two models can be combined by means of the predicted saturation depth (z), to relate the contributing drainage area (A), assumed to be the entire source area, to the local valley gradient ($\tan \theta$) and the angle of internal friction of the soil (ϕ):

$$A = (\rho_s / \rho_w)(K / R_0)zW \sin^2 \theta [(1/\tan \theta) - (1/\tan \phi)] \quad (1)$$

where ρ_s , ρ_w , K , W and R_0 , are, respectively, the saturated bulk density of the soil, the fluid density, saturated hydraulic conductivity, width of the sub-surface runoff zone at the channel head and the steady-state rainfall generating the runoff. Equation (1) is valid only if pressures are hydrostatic and if the slope is less steep than the angle of internal friction, that is, when $[(\rho_s - \rho_w) / \rho_s] \tan \phi < \tan \theta \leq \tan \phi$.

All of these parameters except R_0 can be estimated from field observations and laboratory tests; at present R_0 must be a best-fit parameter in the model (D.R.M. and W.E.D., manuscript in preparation). For the Marin County study area the fitted R_0 has the value 8.5 mm h^{-1} , and equation (1) predicts a strong decrease in source area with increasing gradient (Fig. 1c), similar to that observed in the field data. Equation (1) also implies that a large variance in the source area gradient should be expected because the strength and saturated conductivity of the soil may vary considerably between sites. Because the channel head is displaced downslope when landslide scars infill, the time since the last landslide event at a site will also contribute to this variance.

Contrary to the inverse relationship observed for the data from steep slope gradients, one of the channel initiation theories predicts that in gentle valleys, where channel initiation is due to saturation overland flow²⁵, source areas will be positively correlated with valley gradient. This discrepancy suggests that further work is needed to refine channel initiation theories for shallow-gradient slopes, for which landsliding is uncommon.

Collectively, our data define a strong inverse linear trend over their full range (Fig. 1d). Within this general trend, however, the southern Sierra Nevada data generally plot above data from the Marin County study area, which, in turn, plot above the Coos Bay data. Although many other differences exist between the study areas, this sequence correlates with the variation in mean annual precipitation: 260 mm in the southern Sierra, 760 mm in Marin County and 1,500 mm in the Coos Bay area. Because runoff must increase with increasing drainage area, we suggest that for a given local slope, the source area size required to initiate a channel should increase with increasing aridity to produce the same critical combination of runoff and local slope at the channel head. This hypothesis has important implications for interpreting the response of low-order streams to climatic change. Smaller source areas in wetter regions suggest that channel heads would advance downslope in response to increased aridity, resulting the aggradational infilling of the upper reaches of former first-order channels²⁷. Similarly, channel heads would be expected to advance upslope into colluvial deposits during wetter periods.

Although most channel network evolution models assume that network growth occurs by branching and extension of network tips, the observation that many of the hillside channels in both the Tennessee Valley and southern Sierra areas are discontinuous suggests that channel head locations in these areas are generally controlled by hillslope processes. Furthermore, the inverse relationship of the field data indicates that drainage density should increase significantly with mean landscape gradient. In essence, the smooth, long hills typical of low relief areas result from the large source area required to initiate a channel, whereas the dissected terrain typical of steeper areas reflects the smaller source areas required to sustain channel processes.

We thank Preston Jordan, Anne Bikié, Kent Rich and Yutaka

Komatsu for providing field assistance and Steve Reneau, Peter Whiting, Tom Dunne and Jim Kirchner for constructive comments. We also thank Bill Rankin, the Weyerhaeuser Corporation and the Golden Gate National Recreation Area for access for our study areas. This research was supported in part by a NSF grant and matching funds from the Weyerhaeuser Corporation.

Received 6 June; accepted 5 October 1988.

1. Leopold, L. B. & Langbein, W. B. *U.S. Geol. Surv. prof. Paper 500A* (1962).
2. Howard, A. D. *Geogr. Anal.* **3**, 29–50 (1971).
3. Abrahams, A. D. *Geol. Soc. Am. Bull.* **83**, 1523–1530 (1972).
4. Kirby, M. J. in *Thresholds in Geomorphology* (eds Coates, D. R. & Vitek, J. D.) 53–73 (Allen & Unwin, Boston, 1980).
5. Kochel, R. C., Howard, A. D. & McLean, C. in *Models in Geomorphology* (ed. Woldenberg, M. J.) 313–341 (Allen & Unwin, Boston, 1985).
6. Dunne, T. & Aubry, B. in *Hillslope Processes* (ed. Abrahams, A. D.) 31–53 (Allen & Unwin, Boston, 1986).
7. Willgoose, G. R., Bras, R. L. & Rodriguez-Iturbe, I. *EOS* **69**, 345 (1988).
8. Beven, K. J. & Kirby, M. J. *Hydrol. Sci. Bull.* **24**(1), 43–69 (1979).
9. Leopold, L. B. & Miller, J. P. *U.S. Geol. Surv. prof. Paper 282-A* (1956).
10. Morisawa, M. *EOS* **38**(1), 86–88 (1957).
11. Maxwell, J. C. *Tech. Rep. 19, Off. Nav. Res. Proj. 389-042* (1960).
12. Mark, D. M. A. *Ass. Am. Geogr.* **73**, 358–372 (1983).
13. Dietrich, W. E., Reneau, S. L. & Wilson, C. J. *Proc. Int. Symp. Erosion Sedimentation Pacific Rim*, publ. no. 165, 27–37 (Int. Ass. Hydrol. Sci., 1987).
14. Dietrich, W. E., Wilson, C. J. & Reneau, S. L. in *Hillslope Processes* (ed. Abrahams, A. D.) 361–388 (Allen & Unwin, Boston, 1986).
15. Horton, R. E. *EOS* **13**, 350–361 (1932).
16. Kirby, M. J. & Chorley, R. J. *Bull. Int. Ass. Sci. Hydrol.* **12**, 5–21 (1967).
17. Dunne, T. & Black, R. D. *Wat. Resour. Res.* **6**, 1296–1311 (1970).
18. Beaulieu, J. D. & Hughes, P. N. *Bull. Oregon Dept. Geol. Min. Ind.* **87** (1975).
19. Ruffner, T. A. *Climates of the States* (Gale Research Co., Detroit, 1985).
20. Calif. Div. Min. & Geol. *Geologic Map of California Bakersfield Sheet* (1964).
21. U.S. Geol. Surv. *Topographical Instructions 1B4* (1952).
22. Wahrhaftig, C. in *Franciscan Geology of Northern California* (ed. Blake, M. C.) 31–50 (Soc. Econ. Paleontol. & Min., Los Angeles, 1984).
23. Rantz, S. E. *U.S. Geol. Surv. HA 298* (1968).
24. Hack, J. T. *U.S. Geol. Surv. Prof. Paper 294B* (1957).
25. Kirby, M. J. in *Geomorphological Models* (ed. Ahnert, F.) 1–14 (Cremlingen, FRG, 1987).
26. Iida, T. *Trans. Jap. Geom. Un. S.* **5**, 1–12 (1984).
27. Reneau, S. L., Dietrich, W. E., Dorn, R. I., Berger, C. R. & Rubin, M. *Geology* **14**, 655–658 (1986).

Asthenospheric viscosity inferred from correlated land–sea earthquakes in north-east Japan

Paul A. Rydelek & I. Selwyn Sacks

Department of Terrestrial Magnetism, Carnegie Institution of Washington, 5241 Broad Branch Road, Washington, DC 20015, USA

The viscosity of the Earth's mantle has been estimated from studies of post-glacial rebound^{1,2}, post-seismic deformations of the ground following large earthquakes^{3,4}, and aftershock sequences^{5–7}. Here we derive a value for the viscosity of the asthenosphere from a correlation found in the historical catalogue of subduction-induced seismicity between the intraplate (land) and interplate (sea) earthquakes in north-east Japan. The correlation persists since the time of reliably reported earthquakes in AD 1600; land events precede sea events by ~36 yr, with a mean distance between land–sea pairs of ~200 km. Because of the viscoelastic coupling of the lithosphere to the asthenosphere, a plausible mechanism to explain the correlation is stress migration, governed by the viscosity of the asthenosphere. Large land shocks generate diffuse-like stress pulses which sweep past, and unlock, the thrust fault in the subduction zone, thus triggering the sea events. The correlation time and distance provide a measure of the speed of diffusion (5.6 km yr^{-1}) and hence an estimate of the viscosity ($7 \times 10^{18} \text{ Pa s}$).

The historical catalogue was obtained from a map by the Japanese Meteorological Agency (JMA), which lists the dates, magnitudes, and locations of events of Richter magnitude $M \geq 6.4$ reported since the seventh century AD. The JMA map is shown in Fig. 1 along with major subduction zones in the vicinity of Japan; these subduction zones are associated with active seismic regions, as is generally the case elsewhere. The reporting of earthquakes in the distant past, and the location and intensity